Evidence of internal electric fields in $GaInP_2$ by scanning capacitance and near-field scanning optical microscopy

J-K. Leong and C. C. Williams
Department of Physics, University of Utah, Salt Lake City, Utah 84112

J. M. Olson
National Renewable Energy Laboratory, Golden, Colorado 80401

(Received 31 January 1997)

$GaInP_2$ is studied in cross section with the scanning capacitance and near-field scanning optical microscope. Our study shows significant differences in the electronic and optical properties between ordered single- and two-variant $GaInP_2$. In single-variant samples, spatially uniform capacitance signal, photoluminescence intensity, and band gap are observed. In contrast, a spatially nonuniform capacitance signal, photoluminescence intensity, and band gap are observed in samples with nominally uniform doping. Imaging of the same regions by scanning capacitance and near-field scanning optical microscopes demonstrates that the photoluminescence (observed by the near-field scanning optical microscope) comes only from the n-type-like regions (observed by the scanning capacitance microscope) in lightly doped (n-type) two-variant $GaInP_2$. The local capacitance and photoluminescence measurements can be explained by the presence of internal electric fields in two-variant $GaInP_2$. [S0163-1829(97)07127-0]

I. INTRODUCTION

The phenomenon of atomic ordering has been observed in a wide range of III-V semiconductor alloys.[1] The most common type of ordering in $GaInP_2$ is the CuPt-type ordering which was observed by Gomyo and Suzuki.[2] In the ideal case, a $(GaP)_1(InP)_1$ superlattice forms along a [111] direction. Ordering causes a reduction of the optical band gap, observed experimentally by Gomyo and Suzuki, and first theoretically explained by Kondow *et al.*[3] It is of particular physical and technological interest because the ordering-induced band-gap reduction can be more than 100 meV (Ref. 4) depending on growth conditions.[5,6] Additionally, Raikh and Tsiper predicted that the interpenetration of two different variants results in an additional reduction of band gap as compared to a single variant.[7] However, a clear understanding of the band structure of ordered $GaInP_2$ has not been established.

Atomic ordering in $GaInP_2$ is identified by the appearance of superspots in transmission electron diffraction (TED) patterns.[2,8] For perfectly ordered $GaInP_2$, the periodicity is doubled along one of the four [111] directions. This corresponds to additional points in the corresponding reciprocal lattice. Only two pairs of additional ''superspots'' in TED patterns have been observed. They correspond to ordering along the $[\bar{1}11]$ and $[1\bar{1}1]$ directions. Samples with ordering in only one direction ($[\bar{1}11]$ or $[1\bar{1}1]$) are called single-variant $GaInP_2$ while those that have domains which are ordered in different directions ($[\bar{1}11]$ or $[1\bar{1}1]$) are called two-variant $GaInP_2$. In two-variant $GaInP_2$, a distribution of submicrometer-sized domains of the two variants is typically seen by transmission electron microscopy (TEM) dark-field imaging.[9] The relative volume of the two ordered variants varies with substrate misorientation. TEM dark-field imaging provides a probe of the distribution of these ordered variants throughout the crystal.[9] A correlation between surface faceting and the two ordered variants was observed by Friedman *et al.*[9] The facets are several micrometers in width, and several tens of micrometers in length.[9] Faceting of the top surface of $GaInP_2$ results in a thickness dependence of the photoluminescence (PL) band gap.[10] Recently, n-type- and p-type-like domains in lightly n-type-doped two-variant $GaInP_2$ were observed by scanning capacitance microscopy (SCM).[11] In this work, we report microscopic imaging results with the near-field scanning optical microscope (NSOM), and correlate them with our previous SCM results.[11] Our NSOM results show that the PL intensity and band gap are spatially uniform in lightly doped single-variant $GaInP_2$, while in two-variant $GaInP_2$ they are nonuniform. Direct comparison of NSOM and SCM images demonstrates that the NSOM PL comes only from the n-type-like regions in a lightly n-type-doped two-variant $GaInP_2$ epilayer. These results support the idea that internal electric fields are present in two-variant $GaInP_2$.

II. EXPERIMENTS

A. Samples

Three samples are grown by organometallic vapor-phase epitaxy on (001) GaAs using trimethylindium, trimethylgallium, and PH_3. To produce highly ordered materials, samples are grown at 670 °C. In order to obtain both single- and two-variant $GaInP_2$ samples, the GaAs substrates were misoriented from (001) toward $[\bar{1}10]$ by 4°, 0°, and 2° for samples A, B, and C, respectively.[2,12,13] Sample A is a ($[\bar{1}11]$) single-variant epilayer. Sample B is a two-variant epilayer with the $[\bar{1}11]$ and $[1\bar{1}1]$ variants present in roughly equal amounts. Sample C is a two-variant $GaInP_2$ sample with more of the $[\bar{1}11]$ variant than $[1\bar{1}1]$ variant, as seen by Friedman *et al.*[9] The epilayer thickness of the $GaInP_2$ is ap-

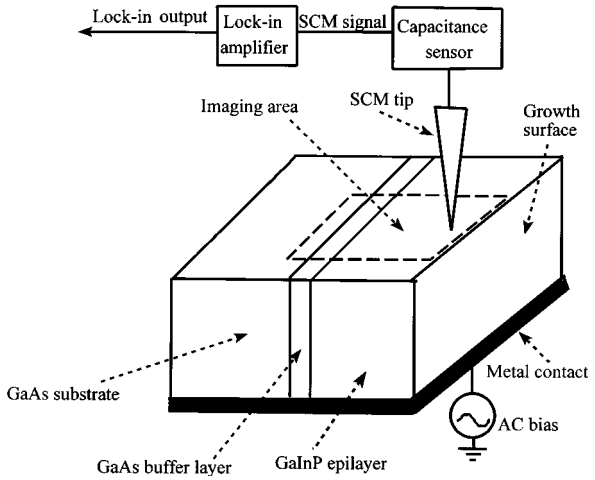

FIG. 1. A sketch of the SCM setup.

proximately 6 μm for samples A and C, and 10 μm for sample B. The thickness of the GaAs buffer layer between the epilayer and the substrate of all samples is approximately 0.6 μm. All $GaInP_2$ epilayers and GaAs buffer layers are nominally undoped, with a typical (unintentional) background doping level of 5×10^{15} cm^{-3} n type for $GaInP_2$ epilayer and 1×10^{15} cm^{-3} p type for GaAs buffer layer, as measured by electrochemical C-V measurements.

B. SCM

A sketch of the SCM experimental arrangement is shown in Fig. 1.[11,14] A metal-coated silicon tip is brought to the surface of the sample and a contact mode atomic force microscope (AFM) is used to maintain the tip-sample distance and scan the tip across the sample. The SCM tip is inductively grounded and a 10–100-kHz ac bias voltage is applied to the sample. The tip-sample capacitance change (ΔC), caused by the applied ac bias voltage, is measured by a high sensitivity capacitance sensor. This change is detected by a lock-in amplifier.

In this experiment, the tip and sample form a MIS (metal-insulator-semiconductor) system. The capacitance-voltage (C-V)characteristics of the MIS system vary depending on the doping concentration, the doping type and the applied voltage.[15] In depletion, the majority carriers are depleted from the semiconductor surface. The total capacitance includes the series capacitance of the insulator and the semiconductor depletion layer. As the applied tip-sample voltage becomes more positive for a n-type semiconductor and more negative for a p-type semiconductor, the depletion layer widens and the depletion layer capacitance falls. Since the insulator capacitance is fixed, the total capacitance also falls. As a result, the slope of the C-V curves of the MIS system has a different polarity for the two types of doping.[15] The experiment was arranged such that a negative lock-in output is observed for p-type samples and a positive lock-in output voltage is observed for n-type samples.

C. NSOM

A sketch of the NSOM experimental arrangement is shown in Fig. 2.[14,16] In the NSOM experiment, an aluminum coated fiber probe[16] is employed as a tip and the tip-sample distance is controlled by shear force microscopy.[17] The excitation mode[14] is used and an Ar^+ (488 nm) laser is used for the excitation. PL images and spectra are taken using a monochromator and an avalanche photodiode with a dark current of eight counts per second. The local PL spectra and PL images are taken from a cleaved (110) surface at room temperature and in air.

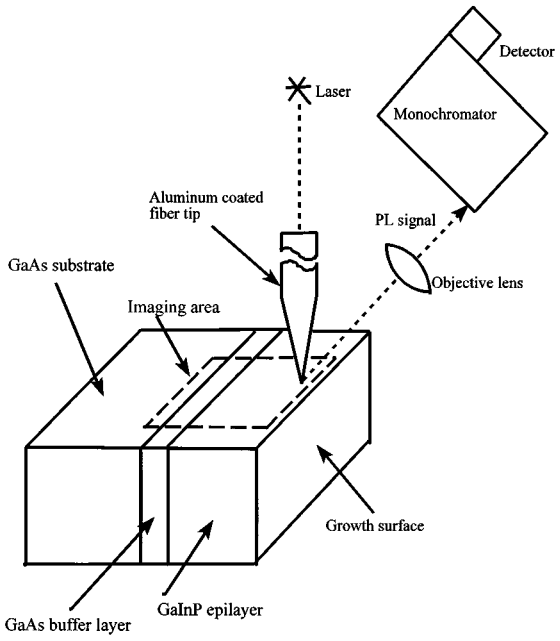

FIG. 2. A schematic diagram of the NSOM used for cross-sectional imaging.

III. RESULTS

A. AFM-SCM results

Single-variant $GaInP_2$ sample (A) and two-variant $GaInP_2$ sample (B) have been imaged by AFM-SCM. Figure 3 shows a capacitance change (ΔC)image on the (110) surface of a cleaved single-variant $GaInP_2$ sample (A). The image area of Fig. 3 is 6×6 μm^2. The topographic variation on

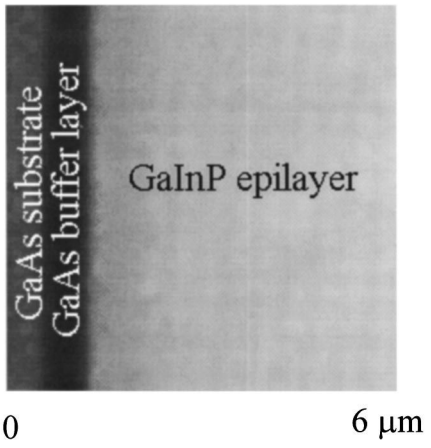

FIG. 3. A capacitance change image of a (110) cross-section surface of a cleaved sample A (single-variant $GaInP_2$).

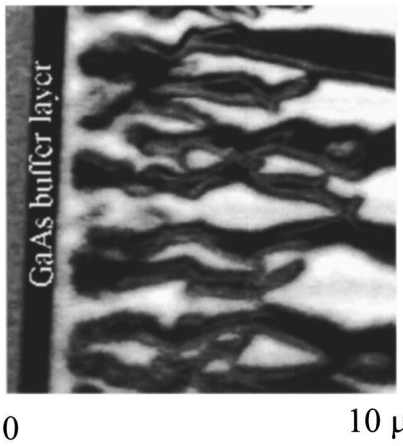

FIG. 4. A capacitance change image of a (110) cross-section surface of a cleaved sample B (two-variant $GaInP_2$).

the cleaved surface is less than 2 nm. The applied ac and dc bias between the SCM tip and the sample are a 2-V peak at 98 kHz, and 0 V, respectively. In Fig. 3, the dark color represents p-type C-V behavior, which corresponds to negative lock-in output signal and the light color represents n-type C-V behavior which corresponds to positive lock-in output signal. The GaAs buffer layer is seen as a nearly vertical dark strip (p type) on the left side of Fig. 3 with a thickness of 0.6 μm. The GaAs substrate, left of the GaAs buffer layer in Fig. 3, shows a uniform small positive lock-in output signal, which agrees with its n-type doping. The $GaInP_2$ epilayer, right of the GaAs buffer layer in Fig. 3, shows very uniform n-type capacitance change, which agrees with its n-type background doping, measured by an electrochemical C-V technique.

Figure 4(a) shows the capacitance change image (10×10 μm^2) on a cleaved (110) surface of the two-variant $GaInP_2$ sample (B). The topographic variation on the cleaved surface is less than 2.5 nm. The applied ac and dc biases between the SCM tip and the sample are a 2-V peak at 98 kHz, and 0 V, respectively. The $GaInP_2$ epilayer, to the right of the GaAs buffer layer in Fig. 4, shows a very nonuniform capacitance change. Both light color (n-type-like) and dark color (p-type-like) regions appear in this epilayer, which is unintentionally doped n type. The n-type- and p-type-like regions are typically smaller near the GaAs buffer layer and larger near the top surface. The spaghetti like regions (approximately zero lock-in output signal) between the n-type- and p-type-like regions may correspond to intrinsic or built in depletion regions, but are not fully understood at this time.

C-V curves on many different locations of the two-invariant $GaInP_2$ sample (B) were observed by SCM. Figures 5(a) and 5(b) show typical C-V curves of the p-type (dark) and n-type (light) like regions, respectively. The C-V curves are similar to high-frequency MIS C-V curves with some characteristic differences. The C-V curve in Fig. 5(a) appears stretched out, i.e., the transition region between accumulation and inversion is not as abrupt as might be expected for this doping level. This could be due to surface states on the $GaInP_2$ surface.[15] As the tip bias voltage is changed, the band bending in the $GaInP_2$ changes, allowing for charge capture and release from the surface states. This process affects the C-V curve shape by stretching out transition region between accumulation and inversion. The C-Vcurve in Fig. 5(b) is shifted along the positive voltage axis. This could be due to charge trapped at $GaInP_2$ surface. It was very difficult to get into accumulation on this sample. This is likely due to leakage current which flows between the SCM tip and sample during measurement.

The SCM images (Figs. 3 and 4) indicate that electronic surface properties are uniform in the single-variant sample, and nonuniform in the two-variant sample, respectively. Many observations on other samples give similar results.

The growth (top) surface topography on the two-variant $GaInP_2$ sample (B), observed by the AFM, is shown in Fig. 6.[9,10] It is composed of distinct hillocks. The facets of hillocks are planes tilted $\sim4°$ from (001) toward $(\bar{1}11)$ and $(1\bar{1}1)$.[10] The facets are several micrometers in width and several tens of micrometers in length. In order to correlate the n-type- and p-type-like regions on a cleaved (110) surface and the top surface structure of the (001) surface, a cross-sectional sample is tilted approximately at an angle of 45°, and the tip is scanned across the cleaved edge. Under this arrangement, the topographic and capacitance change image from both the cleaved (110) cross section and (001) top sur-

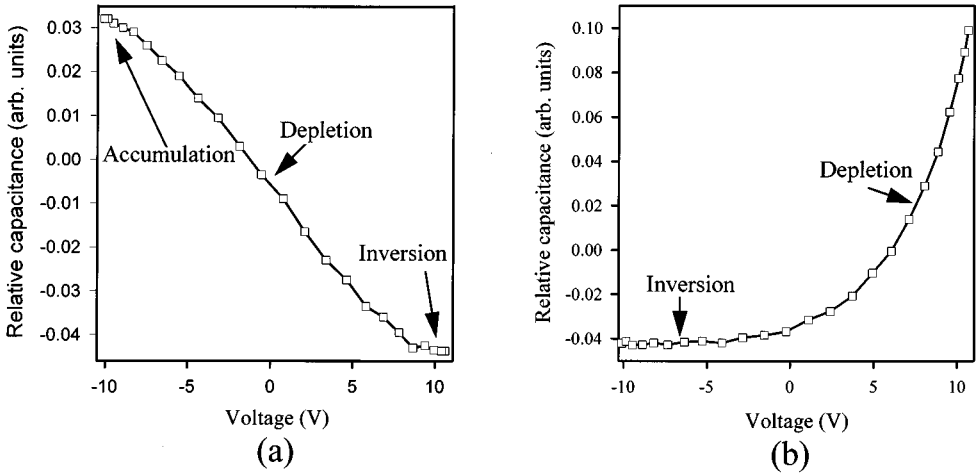

FIG. 5. (a) and (b) C-V curves of p-type- and n-type-like regions of Fig. 4, respectively.

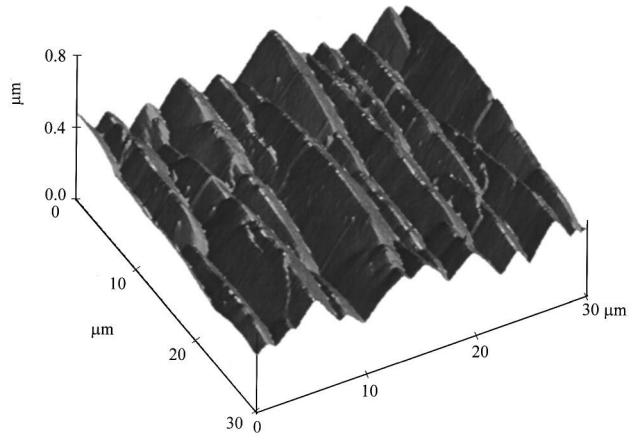

FIG. 6. An AFM image of the surface topography of sample B (two-variant $GaInP_2$).

face can be obtained simultaneously and directly correlated. The capacitance change on the (110) surface and top surface structure (hillocks) of the (001) surface are compared directly at the interface. More than ten different locations were imaged in this mode. We found that the *n*-type- and *p*-type-like regions are all centered under the peaks and valleys of the top surface hillocks, respectively. This establishes a relation between *n*-type- and *p*-type-like regions and the top surface structures. Friedman *et al.* established the correlation between the surface facets and the two different variant domains of the sample.[9] A schematic of these relationships are illustrated in Fig. 11(c).

B. NSOM results

The local PL intensity and band gap of single- (sample A) and two-variant (sample B) $GaInP_2$ samples were investigated by NSOM. Figure 7 shows a NSOM PL image of the (110) surface of single-variant $GaInP_2$ (sample A) with the monochromator wavelength fixed at 684 nm with a 3-nm bandwidth. The image area is 6×6 μm^2. The dark area in Fig. 7 represents no PL signal and the light area represents a finite PL signal. The left side of Fig. 7, which is uniformly dark, is GaAs. To the right side of the GaAs is the $GaInP_2$ epilayer which shows a spatially uniform PL intensity. Note that it is similar to the spatially uniform capacitance change on this sample observed by the SCM. PL spectra were taken at ten different positions on the $GaInP_2$ epilayer, and all spectra show the same peak wavelength of 684 nm.

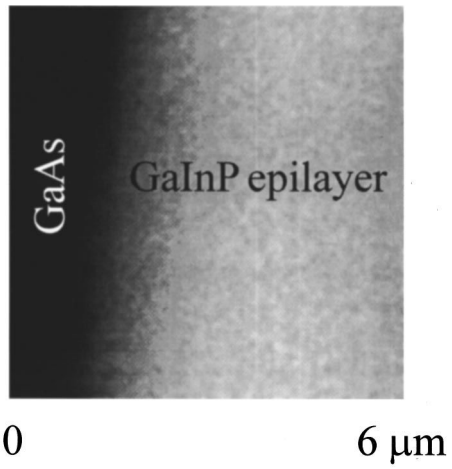

FIG. 7. PL intensity map ($\lambda=684$ nm, 3-nm bandwidth) of cross-sectioned sample A (single-variant $GaInP_2$). The image area is 6×6 μm^2.

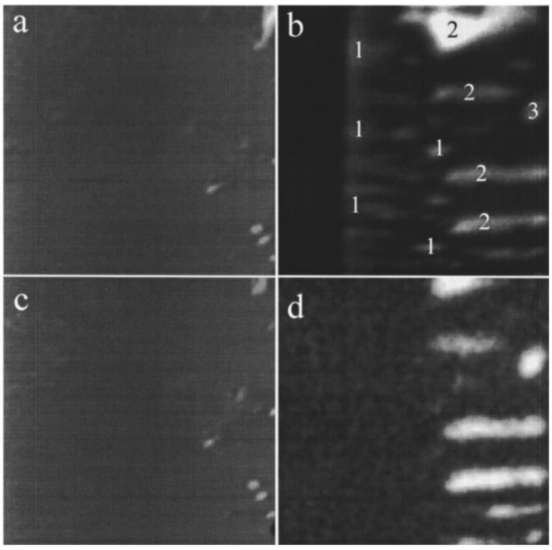

FIG. 8. (a) and (b) Topographic image and simultaneously obtained PL intensity map ($\lambda=670$ nm, 3-nm bandwidth) of cross-sectioned sample B (two-variant $GaInP_2$). (c) and (d) Topographic image and simultaneously obtained PL intensity map ($\lambda=700$, 3-nm bandwidth) of cross-sectioned sample B. The image area is 10.3 by 10.3 μm^2 for all images. All four images have been taken in the same area with the same tip.

In order to compare single- and two-variant $GaInP_2$, a two-variant sample (B) was imaged by NSOM. Figures 8(a) and 8(b) show simultaneously obtained cross-sectional topographic and NSOM PL images of the (110) surface with the monochromator wavelength fixed at 670 nm with a 3-nm bandwidth. The image areas are 10.3×10.3 μm^2. The left side of Fig. 8(b), which is uniformly dark, is GaAs. To the right side of the GaAs is the $GaInP_2$ epilayer, which shows a spatially nonuniform PL intensity. Both light (PL) and dark (no PL) regions appear in this epilayer. The spatially nonuniform PL intensity has the same scale as the nonuniform capacitance change observed on this sample by SCM. The PL-emitting regions of the $GaInP_2$ epilayer are typically small near the GaAs buffer layer and large near top surface. The PL intensity from the $GaInP_2$ epilayer is also weaker near the GaAs substrate and stronger near the top surface. PL spectra were taken at many different positions in Fig. 8(b). Marks 1, 2, and 3 represent positions where the PL spectra are taken, and correspond to the PL spectra 1, 2, and 3 shown in Fig. 9, respectively. Spectrum 3 is amplified by a factor 7 relative to the other spectra. Regions near the GaAs substrate emit PL spectrum 1, and regions near the top surface emit PL spectrum 2. Only one region near the top surface is found to emit PL spectrum 3. The PL band gap in the $GaInP_2$ epilayer is generally larger near the GaAs substrate, and smaller near the top surface. This can be easily seen by comparing Figs. 8(b) and 8(d). Figures 8(c) and 8(d) are simultaneously obtained cross-sectional topographic and NSOM PL images of

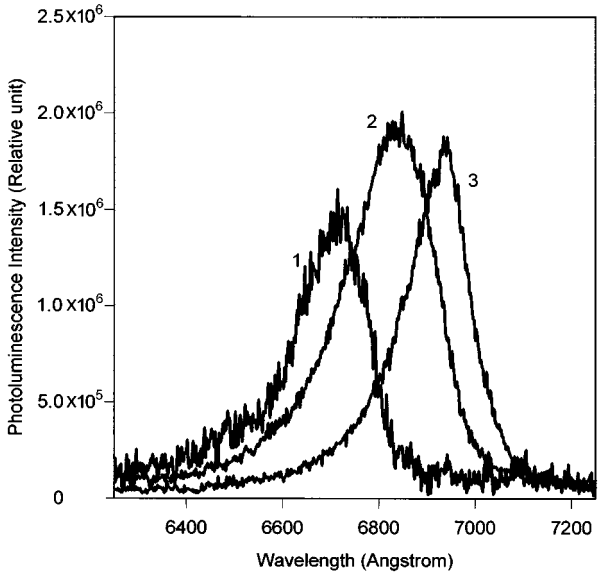

FIG. 9. Near-field PL spectra obtained from three different positions on sample B (two-variant $GaInP_2$) as shown in Fig. 8(b).

the (110) surface with the monochromator wavelength fixed at 700 nm with a 3-nm bandwidth. There is a slight vertical shift of approximately 1 μm between Figs. 8(b) and 8(d). As the comparison between Figs. 8(b) and 8(d) shows, the $GaInP_2$ near the GaAs epilayer emits more light at the shorter wavelengths (670 nm) than at the larger wavelength (700 nm). These images (Figs. 7 and 8) indicate that both the apparent PL band gap and PL efficiency are spatially uniform in single-variant $GaInP_2$, while both are spatially inhomogeneous in two-variant $GaInP_2$.

C. Combined SCM and NSOM results

In order to correlate the PL-emitting regions directly with the n-type- and p-type-like regions in two-variant $GaInP_2$, we scanned an identical area of sample C by SCM and NSOM. The results are shown in Fig. 10. Figure 10(b) shows a SCM image (6.5×8 μm^2) of sample C. The light regions represent n-type-like $GaInP_2$ and the black regions represent p-type-like $GaInP_2$ in this image. Figure 10(d) shows a PL image (6.5×8 μm^2) of sample C in the same location as Fig. 10(b). The light regions represent the PL intensity, and the black regions represent no PL signal in this image. The corresponding topographic images are shown in Figs. 10(a) and 10(c). Figures 10(a) and 10(c) show a slight shift and rotation between the two imaged regions. Marks 1–8 (n-type-like regions) in Fig. 10(b) are in the same relative locations as the marks 1–8 (PL-emitting regions) in Fig. 10(d), respectively, indicating that the *PL comes from the n-type-like regions*. We have imaged four different regions on sample C with similar results.

Note that samples B and C both show n- and p-type regions because both are two-variant samples. However, it is easily observed that the (n- and p-type) structure is different in samples B and C. This is caused by the different growth conditions associated with the different substrate misorientation for samples B and C. Similar variations are seen on different facets of the same samples. We are currently studying these effects.

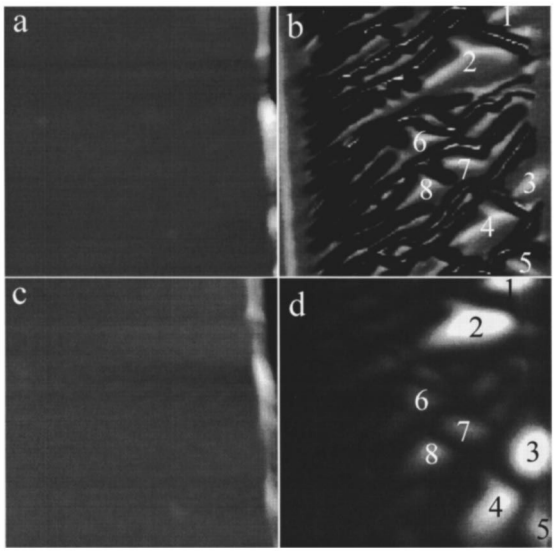

FIG. 10. (a) and (b) Topographic image and simultaneously obtained SCM image of cross-sectioned sample C (two-variant $GaInP_2$). (c) and (d) Topographic image and simultaneously obtained PL intensity map ($\lambda=677$ nm, 3-nm bandwidth) of cross-sectioned sample C. The image area is 6.5×8 μm^2 for all images. All images have been taken in the same area.

IV. DISCUSSION

Figure 11(a) shows a schematic diagram of an idealized (110) cross section of a two-variant $GaInP_2$ epilayer (see Fig. 6).[9] The figures show the topographic and crystallographic structure of the $GaInP_2$ epilayer, with equal quantities of both variants. Friedman *et al.* have shown that variant 1 ($[\bar{1}\bar{1}1]$ variant) sits below facet 1, and variant 2 ($[\bar{1}11]$ variant) sits below facet 2, as shown in Fig. 11(a).[9] Diagonal lines oriented to upper left and upper right corner represent variants 1 and 2, respectively, in Fig. 11(a).

Our explanation for the n-type- and p-type-like domains is that electric fields are present in two-variant $GaInP_2$.[11]

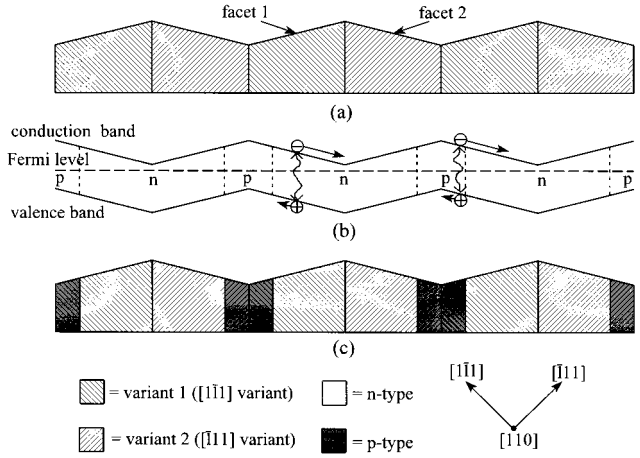

FIG. 11. (a) A sketch of the idealized (110) cross section through the (001) surface. Variant 1 sits below the facet 1, and variant 2 sits below facet 2. (b) A qualitative sketch of the band diagram corresponding to (a) using internal electric fields. (c) Correlation between the n- and p-type regions and topography.

These fields cause band bending, which modulates the local carrier density. There are two possible sources of these electric fields. The first is a strong macroscopic electric polarization along the ⟨111⟩ directions due to ordering in $GaInP_2$.[18,19] Froyen, Zunger, and Mascarenhas calculated that an internal electric field along ⟨111⟩ in ideally ordered $GaInP_2$ may be as large as 16 mV/Å at 0 K.[19] Using this calculation, the internal electric field is along $[1\bar{1}1]$ in variant 1, and along $[\bar{1}11]$ in variant 2 as shown in Fig. 11(a). The $[\bar{1}10]$ component of the fields in variants 1 and 2 point to the left and right, respectively, in this figure. These fields are reflected in the bending of the conduction and valence bands, as shown in Fig. 11(b). Figure 11(b) is the band diagram corresponding to Fig. 11(a) with the internal electric fields present, but neglecting screening by carriers. At the peak of the hillock, the conduction band is near the Fermi level, while near the valley, the valence band is near the Fermi level. If the band bending is significant enough, the intrinsic level will cross the Fermi level and both n-type- and p-type-like regions will show up in the two-variant sample as shown in Fig. 11(c). Figure 11(c) is drawn using the band structure in Fig. 11(b). The white and gray regions represent the n-type- and p-type-like regions, respectively. The n-type regions appear below the peaks of hillocks, and the p-type regions appear below the valleys of the hillocks. This model explains the appearance of n- and p-type regions in two-variant $GaInP_2$, and is consistent with our SCM experimental results. Note that the [001] component of the field in variants 1 and 2 is in the same upward direction. We believe that this component of the internal electric field will be screened by charges at the top surface and free carriers from the substrate at the $GaInP_2$/GaAs interface. In single-variant $GaInP_2$, the internal electric field along the upward ([001]) direction will be canceled by surface and substrate charges in a similar manner. The field along the [110] direction, however, is very small because the polarization charges are separated by the single-variant domain size, which is comparable to the sample size. Therefore, polarization-induced band bending in single-variant $GaInP_2$ will not be seen by the SCM.[19]

The other possible source for internal electric fields is dopant segregation[20,21] on the nonplanar surfaces of two-variant samples (see Fig. 5). Our results could be explained by segregation of n- and p-type dopants during growth on the peaks and valleys of hillocks, respectively, in two-variant $GaInP_2$. Because single-variant samples typically have a planar surface, such dopant segregation should not occur, consistent with a uniform SCM signal, as observed. We cannot conclude here whether the internal electric field is a polarization effect or due to dopant segregation. Further work is in progress.

The spatially nonuniform PL on two-variant $GaInP_2$ (samples B and C) can also be explained using the band bending model proposed to explain our SCM results, as shown in Fig. 11(b). In these samples, there are three reasons that more PL is emitted from the n-type-like regions than the p-type-like regions. The first is that the magnitude of the carrier concentration in the n-type- and p-type-like regions is different. Samples B and C were nominally undoped, but have an n-type background doping as measured by electrochemical C-V measurements and known from growth data. This means that the average Fermi level is closer to the conduction band than the valence band. Therefore, the electron concentration in the middle of the n-type-like regions is greater than the hole concentration in the middle of p-type-like regions. Because the PL radiative recombination rate should increase with the local concentration of majority carriers, the PL intensity in the n-type-like regions should be higher than that of p-type-like regions. Second, the mobility of electrons is higher than that of holes in $GaInP_2$. In the n-type-like region, a hole [as shown in Fig. 11(b)], generated by pump light, will drift toward the adjacent p-type-like region because of the electric field present in this region. The rate at which the holes will recombine with conduction electrons in the n-type-like region depends upon how fast a hole drifts. A similar situation exists in the p-type-like region. Since in $GaInP_2$ the mobility of electrons is higher than that of holes, the chance of the hole recombining with a conduction electron in the n-type-like region is higher than that of the electron recombining with a hole in the p-type-like region. A third fact may also explain our observations. Where the majority-carrier concentration is high, more screening of the internal electric field will occur. In such a region, minority carriers will have a small drift velocity and thus a higher probability of emitting PL. Since the majority-carrier concentration in the n-type regions is higher than that of the p-type regions (for n-type background-doped samples), the p-type regions will have a larger drift field than that of the n-type regions. As a result, the recombination rate in the p-type-like regions will be lower than that of the n-type-like regions. All three of the arguments above indicate that the n-type-like regions should emit more PL than the p-type-like regions, as seen in the experimental results shown in Fig. 10.

We observe that the PL-emitting regions (n type) in the $GaInP_2$ epilayer are smaller near the GaAs substrate than near the top surface in samples B and C. This can be explained by the fact that the growth facets, related to two-variant domains,[9] become larger with increasing epilayer thickness in two-variant $GaInP_2$. Therefore n-type-like regions (PL-emitting regions), directly related to two variant domains, also become larger with increasing epilayer thickness. The PL intensity from the $GaInP_2$ epilayer is observed to be weaker near the GaAs than near the top surface as well. This can be explained by the fact that domain walls may serve as nonradiative recombination centers. The ratio of domain-wall area to the domain volume will be larger for smaller domain sizes. Therefore, nonradiative recombination is more likely near the GaAs substrate than near the top surface. The peak PL emission energy from the $GaInP_2$ near the GaAs is also larger than near the top surface in samples B and C. This is a result similar to that measured by Friedman *et al.*[10] This observation is probably due to an increase in the degree of order with epilayer thickness.[10] It is not likely due to the presence of internal electric fields in two-variant $GaInP_2$. As the thickness of the $GaInP_2$ epilayer increases, growth surface facets of hillocks are formed in two-variant $GaInP_2$. These facets develop and finally reach 4° from (001) toward the $(\bar{1}11)$ and $(1\bar{1}1)$ planes. The $GaInP_2$ grown on these $\pm 4°$ facets sees the same growth condition as $GaInP_2$ grown on 4° misoriented substrates, which gives single-variant $GaInP_2$ and minimum band gap.[10] This is the reason

that the peak PL band gap of $GaInP_2$ near the GaAs substrate is higher than that of $GaInP_2$ near the top surface in samples B and C.

V. CONCLUSIONS

In summary, we have imaged the (110) surfaces of cleaved $GaInP_2$ by SCM and NSOM. A uniform n-type SCM signal is observed in lightly n-type-doped single-variant $GaInP_2$, and both n-type- and p-type-like structures appear in lightly n-type-doped two-variant $GaInP_2$. The PL intensity and band gap are uniform on single-variant $GaInP_2$. In two-variant $GaInP_2$, the PL intensity is spatially nonuniform and the apparent band gap of the $GaInP_2$ near the substrate is higher than that of $GaInP_2$ near the top surface. Same-area imaging by SCM and NSOM on two-variant $GaInP_2$ with an n-type background doping shows that the PL comes from the n-type-like regions. All of these results support the model that internal electric fields are present in two-variant $GaInP_2$.

ACKNOWLEDGMENTS

The authors from University of Utah thank S. Froyen, M. Raikh, E. Rashba, J. Worlock, M. C. DeLong, J. McMurray, C. Inglefield, and P. C. Taylor for helpful discussions and suggestions. J. M. O. is grateful to M. C. DeLong, Sarah R. Kurtz, and D. J. Friedman for helpful discussions, and to Charlene Koomer, who helped with the sample preparation and characterization. J. M. O. wishes to thank the Office of Energy Research Materials Science Division of the DOE for financial support of this work.

[1] G. B. Stringfellow and G. S. Chen, J. Vac. Sci. Technol. B **9**, 2182 (1991).
[2] A. Gomyo, T. Suzuki, and S. Iijima, Phys. Rev. Lett. **60**, 2645 (1988).
[3] A. Gomyo, T. Suzuki, K. Kobayashi, S. Kawata, I. Hino, and T. Yuasa, Appl. Phys. Lett. **50**, 673 (1988); M. Kondow, H. Kakibayashi, S. Minagawa, Y. Inoue, T. Nishino, and Y. Hamakawa, J. Cryst. Growth **93**, 412 (1988).
[4] M. C. DeLong, P. C. Taylor, and J. M. Olson, Appl. Phys. Lett. **57**, 620 (1990).
[5] T. Suzuki, A. Gomko, S. Iijima, K. Kobayashi, S. Kawata, I. Hino, and T. Yuasa, Jpn. J. Appl. Phys. **27**, 2098 (1988).
[6] S. R. Kurtz, J. M. Olson, and A. E. Kibbler, Appl. Phys. Lett. **57**, 1922 (1990).
[7] M. E. Raikh and E. V. Tsiper, Phys. Rev. B **49**, 2509 (1994).
[8] P. Bellon, J. P. Chevalier, G. P. Martin, E. Dupont-Nivet, C. Thiebaut, and J. P. Andre, Appl. Phys. Lett. **52**, 567 (1988).
[9] D. J. Friedman, J. G. Zhu, A. E. Kibbler, J. M. Olson, and J. Moreland, Appl. Phys. Lett. **63**, 1774 (1993).
[10] D. J. Friedman, G. S. Horner, Sarah R. Kurtz, K. A. Bertness, J. M. Olson, and J. Moreland, Appl. Phys. Lett. **65**, 878 (1994).
[11] J-K. Leong, C. C. Williams, J. M. Olson, and S. Froyen, Appl. Phys. Lett. **69**, 4081 (1996).
[12] P. Bellon, J. P. Chevalier, E. Augarde, J. P. Andre, and G. P. Martin, J. Appl. Phys. **66**, 2388 (1989).
[13] T. Suzuki, A. Gomyo, and S. Iijima, J. Cryst. Growth **93**, 396 (1988).
[14] J-K. Leong, J. McMurray, C. C. Williams, and G. B. Stringfellow, J. Vac. Sci. Technol. B **14**, 3113 (1996).
[15] S. M. Sze, *Physics of Semiconductor Devices*, 2nd ed. (Wiley, New York, 1981), Chap. 7.
[16] E. Betzig and J. K. Trautman, Science **257**, 189 (1992).
[17] J.-K. Leong and C. C. Williams, Appl. Phys. Lett. **66**, 1432 (1995).
[18] R. G. Alonso, A. Mascarenhas, G. S. Horner, K. Sinha, J. Zhu, D. J. Friedman, K. A. Bertness, and J. M. Olson, Solid State Commun. **88**, 341 (1993).
[19] S. Froyen, A. Zunger, and A. Mascarenhas, Appl. Phys. Lett. **68**, 2852 (1996).
[20] M. Kondo, C. Anayama, N. Okada, H. Sekiguchi, K. Domen, and T. Tanahashi, J. Appl. Phys. **76**, 914 (1994).
[21] T. Y. Wang, L. S. Heath, and W. Stutius, Appl. Phys. Lett. **63**, 755 (1993).